Research Article

Journal of Environmental Nanotechnology

Enhancement of Mechanical and Wear Properties in 3D-printed PEEK Specimens using Eco-friendly Infill Patterns via Fused Filament Fabrication

Rajeshkumar Dhanapal[1], Vasudevan Alagumalai[1*], Y. Justin Raj[1], Sundarakannan Rajendran[1] and Justin Sam George[2]

[1]Department of Mechanical Engineering, Saveetha School of Engineering, Saveetha Institute of Medical and Technical Sciences, Saveetha University, Chennai, TN, India

[2]Department of Civil Engineering, RWTH AACHEN University, Aachen, North Rhine-Westphalia, Germany

Received: 07.08.2024 Accepted: 12.12.2024 Published: 30.12.2024

*avasudevan.phd@gmail.com

ABSTRACT

The increasing use of 3D-printed PEEK materials in load-bearing applications necessitates a comprehensive evaluation of their wear characteristics and hardness under dynamic loading conditions. This study investigates the wear loss, coefficient of friction, and hardness values of PEEK materials with four distinct surface patterns: Line, Grid, Cubic, and Hexagon. Controlled experiments revealed that the Line and Hexagon patterns exhibited the lowest wear loss (0.004 grams), indicating superior wear resistance, while the Cubic pattern showed the highest wear loss (0.009 grams). In terms of friction, the Grid pattern demonstrated the lowest coefficient of friction (0.21), suggesting it offers the least resistance to movement, while the Line and Hexagon patterns had moderate coefficients of friction (0.40 and 0.35, respectively). The Cubic pattern displayed the highest coefficient of friction (0.45). Hardness testing revealed that the Hexagon pattern had the highest hardness value (30), followed by the Line pattern (28), the Grid pattern (25), and the Cubic pattern (20). These findings highlight the trade-offs between wear resistance, friction, and hardness among the different surface patterns, providing valuable insights for applications where these properties are crucial. SEM images were analyzed to investigate the wear characteristics of FFF-printed PEEK samples with varying infill patterns. The results showed that the Hexagon pattern exhibited the least surface degradation, demonstrating superior wear resistance compared to the Line, Cubic, and Grid patterns. This study offers valuable guidance for selecting optimal surface patterns in engineering and industrial applications to enhance performance and durability.

Keywords: 3D-printed PEEK; Mechanical properties; Wear properties; Eco-friendly infill patterns; Fused Filament Fabrication (FFF); Surface morphology.

1. INTRODUCTION

Polyetheretherketone (PEEK) has emerged as a preferred material in advanced engineering applications due to its exceptional mechanical properties, thermal stability, and biocompatibility. With the increasing adoption of 3D printing techniques like Fused Filament Fabrication (FFF), optimizing infill patterns has become critical to enhancing the material's performance in load-bearing and wear-intensive environments. the 3D printing industry continues to experience significant growth and innovation, reaching a market value of over $20 billion for the first time. This growth is driven by the transformative impact of 3D printing across various sectors, including aerospace, automotive, electronics, healthcare, and energy, where the technology offers enhanced efficiency, customizability, and cost-effectiveness compared to traditional manufacturing methods. The rise of 3D printing in ceramics, in particular, has opened new possibilities, allowing the fabrication of complex structures and the use of diverse raw materials, overcoming the limitations of conventional fabrication methods (Subramani *et al.* 2024). Traditional 3D printing processes with thermoplastic elastomers face conversion difficulties and uniform extrusion issues, limiting their effectiveness. The 3D printing industry faces several challenges that limit its ability to scale production efficiently, including high material costs, inconsistent part quality, and the need for extensive post-processing (Ree *et al.* 2024). There are concerns about the environmental impact of certain materials and energy consumption (Zhang *et al.* 2024). Challenges around printing speed and quality control, particularly for large-scale 3D printing applications, make it difficult to scale production efficiently. Fused filament fabrication, also known as fused deposition modelling, is a widely used 3D printing technology. It works by extruding melted thermoplastic filament through a heated nozzle, building objects layer by layer (Mehtedi *et al.* 2024). FFF printers are user-

friendly, offering a wide range of materials such as PLA, ABS, and PETG, each with unique properties. Despite its benefits, FFF has notable drawbacks, including visible layer lines and a generally rough surface finish (Kantaros *et al.* 2023). Printing can be slow, especially for large or high-resolution objects, and support structures often increase print times Fused Filament Fabrication (FFF), also known as fused deposition modelling, utilizes a variety of materials to cater to different printing needs and applications. One of the most popular materials is PLA (Polylactic Acid), which is biodegradable and easy to print, making it ideal for beginners and for educational purposes (Kharmanda *et al.* 2023). However, PLA has limited mechanical strength and heat resistance (Hou *et al.* 2023). ABS (Acrylonitrile Butadiene Styrene) is stronger and more heat-resistant than PLA but can be challenging to print due to its tendency to warp and emit odors during printing. ABS is commonly used in automotive parts, toys, and household items. PETG (Polyethylene Terephthalate Glycol) offers a balance by combining the ease of PLA printing with the strength and durability of ABS, making it suitable for functional parts and outdoor use (Durga *et al.* 2023). It is also transparent and can be used for food-safe applications (Sarker *et al.* 2023). Polymer materials are pivotal in modern industry due to their diverse properties and applications. These versatile substances can be tailored to exhibit a wide spectrum of characteristics, from flexibility and elasticity to rigidity and strength (Khan *et al.* 2023). Their lightweight nature contributes to fuel efficiency in aerospace and automotive sectors, while their durability ensures longevity in various applications, resisting wear and corrosion (Khan *et al.* 2024). Polymers are highly processable, enabling cost-effective manufacturing through techniques such as injection molding and 3D printing (Farrugia *et al.* 2024). They serve crucial roles as electrical insulators in electronics and offer biocompatibility for medical implants and drug delivery systems.

Chithambaram *et al.* (2024) examined the hardness and wear behaviour of the polyetheretherketone (PEEK) specimens using a fused deposition modelling approach. The microhardness was measured using Vickers's microhardness tester, and wear behaviour was evaluated using the pin-on-disc method. They suggest that the test specimen created utilizing the parameters, including a printing speed of 20 mm/s and a layer thickness of 0.15 mm, had better wear and hardness properties than the other test specimens.

Dhakal *et al.* (2024) investigated the tribological properties of neat and carbon fiber-reinforced polyether-ether-ketone (PEEK) materials manufactured using the fused filament fabrication (FFF) technology. The reciprocating sliding behavior of printed polymers against stainless steel (SS) was investigated in both dry and water-lubricated circumstances. The findings of this study have implications for enhancing the processing design of PEEK-based materials in extrusion-based 3D printing for tribological purposes.

Haleem *et al.* (2019) studied and examined the coefficient of friction and wear aspects of ABS polymer, with an emphasis on optimal 3D printing parameters. Layer height has a considerable impact on friction and wear rate, according to research using fused filament fabrication and response surface methods using a Box-Behnken design. The ideal settings include a layer height of 0.10 mm, a nozzle temperature of 234℃, and a triangle print pattern. He *et al.* (2023) conducted orthogonal experiments to investigate the impact of annealing temperature and FDM parameters (nozzle temperature, platform temperature, layer thickness, and printing speed) on the mechanical properties of PEEK. With lower elongation at break and a peak in mechanical strength at 300 °C, annealing temperature was found to be positively correlated. The final strengths increased by 36%, 54%, and 21% in the tensile, flexural, and compressive domains. Examined in parallel, PEEK annealed at 200 °C showed the lowest wear rate ($1.37 \times 10{-}6$ mm³/Nm).

Massocchi *et al.* (2021) examined the friction and wear of PEEK in a dry sliding environment (without lubrication) and contrasted with those of Babbitt metal using a ball-on-disk tribometer.PEEK polymers exhibit CoFs of roughly 0.22 and 0.16 under the 1 and 5 N applied stress, respectively, according to the experimental activity's results. Results for CoF and wear volume loss are presented and contrasted with the Babbitt coating used as a reference. The mechanical characteristics of specimens produced by 3D printing technology from poly-ether-ether-ketone material were ascertained, and the impact of print directionality on the mechanical properties was also examined (Mrówka *et al.* 2021). Two populations of specimens were studied; one had a crystal structure, while the other had an amorphous structure. Impact, three-point bending, and static tensile tests were performed. The outcomes show that compared to the unmodified specimens, the changed PEEK specimens have poorer thermoplastic characteristics. Lv *et al.* (2024) studied the new polyether ether ketone (PEEK)-based composites were made using multi-material fused deposition modelling (FDM) and consisted of silicon dioxide-filled and alternating short carbon fiber-reinforced PEEK layers. The combination effect of rolling nanoparticles and graphitized self-lubricating transfer films was discovered to be responsible for the minimal friction and wear that occurred at high contact pressure.

Wang *et al.* (2024) introduced a unique method that produces PEEK with different filling densities using 3D printing technology and then enhances PEEK's frictional performance by conducting in situ synthesis of zeolite imidazole framework (ZIF-8) nanomaterial on its surface. The results show that the composite material

performs significantly better in terms of friction under low load, with a minimum wear rate of 4.68×10^{-6} mm^3/Nm, which is approximately 1.3 times better than the wear rate of 1.091×10^{-5} mm^3/Nm for the non-grafted PEEK material. This study addresses a significant research gap by examining the wear performance of PEEK manufactured through FFF.

Timoumi *et al*. (2022) investigated tensile properties using the Taguchi approach and identified optimal mechanical properties, including a tensile strength of 54.97 MPa and a modulus of 2.67 GPa, achieved with a honeycomb pattern having 40% infill. This configuration also resulted in a maximum stress of 7.186 MPa and a strain of 0.00627 mm, demonstrating potential for lightweight orbital implants. The authors concluded that wear properties could be minimized by optimizing tensile strength and Young's modulus. Similarly, Hassan et al. (2021) employed an experimental design to analyzed infill patterns (rectilinear, grid, triangular, wiggle, fast honeycomb, and full honeycomb) and infill percentages (25%, 50%, 75%, and 100%). Energy consumption (EC) was found to be high for wiggle and triangular patterns and low for the rectilinear pattern during both the printing stage and the overall process. Pulipaka *et al* (2023) measured mechanical properties and observed that roughness tests did not affect hardness and creep. Greco et al. studied the fatigue behavior of FFF-produced PEEK, considering variations in infill patterns (triangular and rectilinear). Specimens with rectilinear patterns exhibited superior fatigue performance, achieving infinite fatigue life at a maximum applied stress around 70% of the ultimate tensile stress. Greco,A et .al (2024) investigated The fatigue behavior of PEEK (Polyether Ether Ketone) made by Fused Filament Fabrication (FFF) is examined in this work, with particular attention to the effects of changes in infill pattern (rectilinear or triangular) and layer height (0.15 mm or 0.25 mm). The results of the fatigue tests indicate that fatigue behaviour is significantly influenced by the infill design, with the rectilinear pattern outperforming the triangular one. When paired with the rectilinear infill pattern, layer height had minimal impact. Better fatigue performance was demonstrated by specimens with rectilinear patterns, which reached infinite fatigue life at about 70% of the ultimate tensile stress.

Specifically, this research investigates how different infill patterns—Hexagon, Grid, Circle, and Line—affect the material's wear behavior. Wear tests were conducted under varying conditions to measure the material's performance. Understanding the interplay between infill patterns and wear performance will enable not only the optimization of infill selection for enhanced durability but also the expansion of the practical uses of 3D printed PEEK components. By elucidating these relationships, the study aims to ensure the reliability and efficiency of 3D printed PEEK in diverse real-world applications, potentially transforming practices in industries where high-performance polymers are required.

2. MATERIALS AND METHODOLOGY

2.1. FFF Printing

This study employed fused filament fabrication (FFF) to print PEEK with several infill patterns, such as Line, Grid, Cubic, and Hexagon. The PEEK material (product code: PEEK K10), which was obtained from Kexcelled3D in China, had the following specifications: density: 1.23 g/cm^3; tensile strength range: 70–80 MPa elongation range: 4-6%. The filament measured 1.75 mm in diameter. India's Creatbot provided the FFF machine. Using Catia V5 software, the design model for 3D printing was produced and saved in STL format. The nozzle used by the FFF machine had a diameter of 0.4 mm. The printing process was carried out at 410°C for the nozzle and 120 °C for the bed in order to improve adhesion and minimize warping. Throughout the printing process, a build orientation of 45°, an infill density of 100%, and a layer height of 0.2 mm were maintained. To guarantee correct adhesion to the build plate, the height of the initial layer was slightly increased to 0.3 mm. In light of the mod's intricacy, the printing speed was set at 30 mm/min in order to balance speed and print quality.

2.2 Experimental Procedure

The mechanical and tribological properties such as hardness and wear loss were calculated as per the ASTM standards.

2.2.1 Wear Test

Fig. 1 illustrates a test setup for evaluating the mechanical properties of materials. Panel (A) shows the overall apparatus, including the component used for sample positioning and feeding. Panel (B) zooms in on the specific section of the setup, where the material sample is being subjected to a test, as indicated by the red arrow. This setup likely involves mechanical testing methods such as wear or friction testing, which can provide insight into the performance of materials under dynamic conditions. During the wear test, the coefficient of friction and wear rate were determined on the four samples of different patterns such as Line, Grid, Cubic and Hexagon.The specimen weight is measured and recorded before and after the test. The difference in weight of the sample is the wear loss. The coefficient of friction and wear rate was calculated using the standard formulas and procedure.

The following equations (1) and (2) can be used for the calculation of both the coefficient of friction and wear rate.

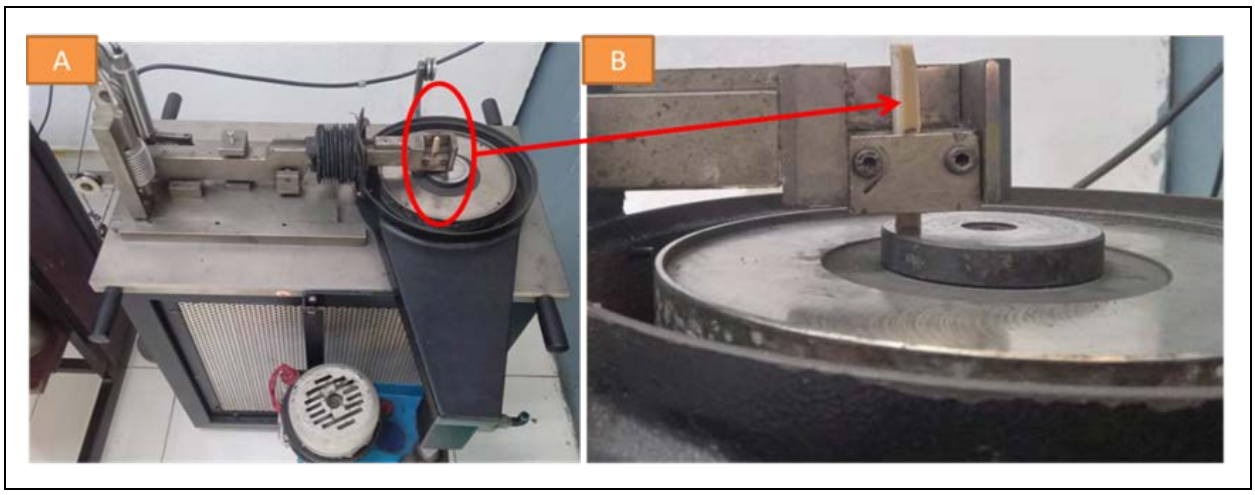

Fig. 1: Pin-on-disc (a) machine setup (b) enlarged view of sample position

$$\text{Coefficient of friction} = Ff/F \quad \ldots (1)$$

Where, Ff – frictional force in N and F – applied load in N.

$$\text{Wear loss in g} = W1-W2 \quad \ldots (2)$$

Where, W1- weight of the sample before test, W2 - weight of the sample after test

Table 1 displays experimental settings for all wear test samples. The purpose of this wear analysis experiment was to asses a material's wear properties under particular operating conditions. The material was subjected to an applied force of 10 Newton's, which replicated the stress it would encounter in practical situations. The relative speed between the material and the counter surface was determined by sliding the substance at a speed of one meter per second. With 500 meters of sliding distance covered in the test, a thorough evaluation of wear across a sizable length was guaranteed. To ensure continuous sliding action, the material was allowed to slide along a 40 mm diameter circular route at a rotating speed of 478 revolutions per minute. 500 seconds were allotted to the test's execution. Throughout the test, data was probably recorded at intervals of 13 minutes and 32 seconds, giving precise insights into the wear behavior. This rigorous methodology contributes useful information for the material's prospective application in many industries by enabling a complete investigation of the material's wear resistance.

Table 1. Experimental settings for all wear test samples

Test Parameters	Machine Settings
Applied load (N)	101
Sliding velocity (m/s)	1
sliding distance (mm)	500
sliding dia (mm)	40
RPM	478
Time	13 minutes and 32 seconds

2.2.2 Hardness Test

The average value of five samples was taken as hardness value of PEEK pattern. In the hardness test, the load is gradually applied on the specimen for penetration in five places, and after some time, the load can be removed and take the average of five indentations on the specimen.

Fig. 2 shows the test samples used during the wear test

3. RESULT AND DISCUSSION

Based on the test results found after conducting wear and hardness tests on the different patterns of the samples have been discussed here.

3.1 Coefficient of Friction and Wear

The Fig. 3(a) illustrates the coefficient of friction over time for four different surface textures Line, Grid, Cubic, and Hexagon, which is crucial for understanding their wear behavior under dynamic conditions. The graph represents the x-axis represents time in (m/s) while the y-axis shows the coefficient of friction. Each texture exhibits an initial transient phase where the coefficient of friction changes rapidly before stabilizing after approximately 100 milliseconds. The hexagon texture shows the highest stabilized coefficient of friction at around 0.45, followed by the line texture at 0.4, the cubic texture at 0.35, and the grid texture at 0.3. These results suggest that surface textures significantly

influence wear behavior, with higher coefficients of friction typically indicating higher wear rates. Consequently, the hexagon texture, despite providing the highest friction, may experience more significant wear compared to the grid texture. This analysis highlights the importance of selecting appropriate surface textures to balance friction and wear for various applications. This investigates how a cell's survival is impacted by the mechanical interaction with its surroundings, quantified by the coefficient of friction.

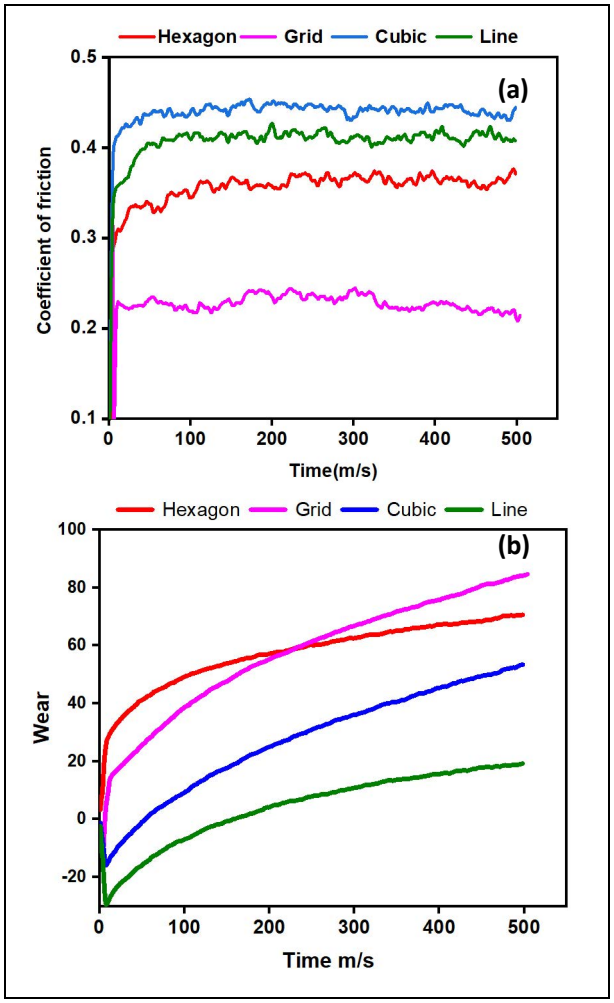

Fig. 3: (a) Represents the coefficient of friction and time and figure (b) Represents the wear and time

The graphs represent the cell's tolerance to these interactions, with the x-axis depicting the coefficient of friction (measured in milliseconds) and the y-axis representing a measure of cell health or survival time. The grid type and line styles differentiate the specific mechanical environments. The top left graph, visualized on a linear grid with a straight line, suggests that a cell on a smooth surface (linear grid) experiences optimal survival (around 500 milliseconds) under low friction (around 0.15). This implies that minimal friction allows the cell to move freely, potentially facilitating essential mechanical processes like nutrient uptake and waste removal, ultimately extending its lifespan. In contrast, the bottom left graph, plotted on a cubic grid with a curved line, indicates that a cell in a more confined environment (cubic grid) survives longest (around 400 milliseconds) under high friction (around 0.40). The increased friction in this scenario might provide crucial mechanical support, preventing excessive movement and potential damage to the cell in a structurally complex environment. The Fig. 3(b) presented on a hexagonal grid with a line labelled "Wear," offers insights into mechanical wear. Here, the y-axis might represent the amount of wear the cell experiences.

This graph suggests that on a honeycomb-like structure (hexagonal grid), the cell experiences the least wear (around 0.20) when the coefficient of friction is high (around 0.40). This implies that high friction in this context reduces the mechanical stress and wear on the cell by providing stability. In conclusion, the figure highlights how the frictional forces acting on a cell, a fundamental mechanical property of its environment, can significantly influence its survival. Understanding this interplay between mechanical properties and cell biology is crucial in areas like bioengineering and tissue regeneration, where designing surfaces that optimize cell function and lifespan requires careful consideration of the mechanical cues.

The table 2 summarizes the results of a wear analysis experiment on different 3D printed patterns. The experiment evaluated the wear resistance of the patterns by measuring their weight loss before and after a simulated wear test.

Table 2. Experimental reading of wear analysis

Patterns	Initial weight (g)	Final weight (g)	Wear loss(g)
Line	1.551	1.547	0.004
Grid	1.437	1.43	0.007
Cubic	1.488	1.479	0.009
Hexagon	1.451	1.447	0.004

As observed, all patterns exhibited some degree of wear loss during the experiment. The cubic pattern showed the highest wear loss (0.009 g), followed by the grid (0.007 g) and the Line and Hexagon patterns (0.004 g each). These initial findings suggest that the geometry of the 3D printed pattern may influence its wear resistance. Further analysis is required to determine the specific mechanisms contributing to wear in each pattern.

The graph from Fig. 4 (a) and (b) presents a technical analysis of the coefficients and wear loss for four different samples: Line, Grid, Cubic, and Hexagon, with associated error bars indicating variability in the measurements. The wear coefficient values are as follows: Line (0.41), Grid (0.22), Cubic (0.42), and Hexagon (0.35). The wear coefficient indicates the rate at which material is worn away under specified

conditions. The relatively high wear coefficient for the Line sample (0.41) suggests moderate resistance to wear, likely due to its uniform but less interlocked microstructure. The Grid sample (0.22) exhibits significantly lower wear, indicating enhanced wear resistance, likely due to better stress distribution and reduced localized deformation.

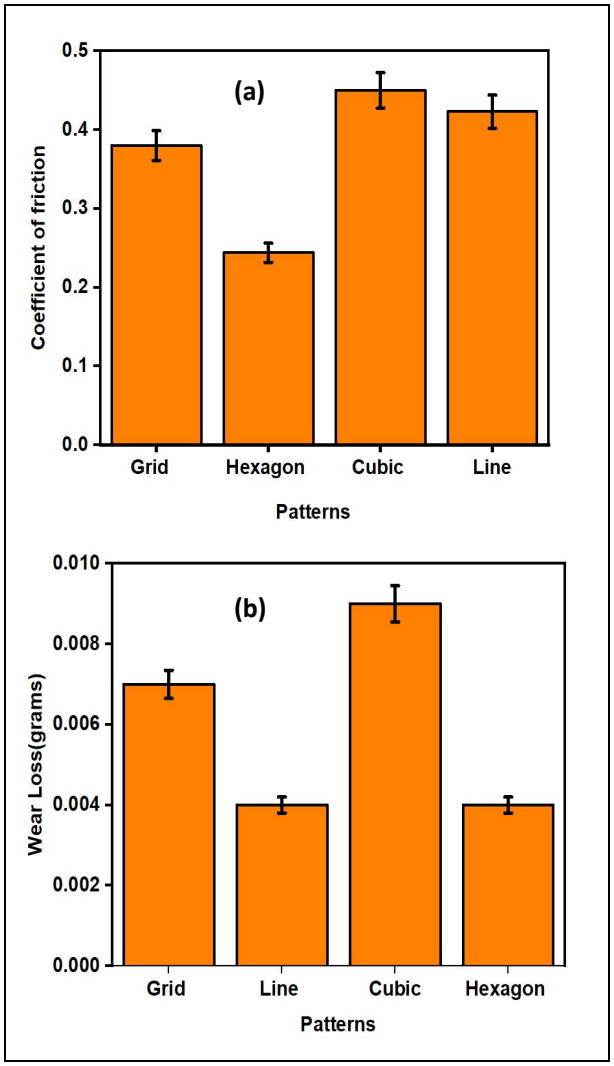

Fig 4(a) displays the coefficient of friction for various infill patterns (b) illustrates the wear loss of various infill patterns

The Cubic sample (0.42) has a wear coefficient similar to the Line sample, suggesting that the cubic geometry does not significantly enhance wear resistance, possibly due to internal stress concentrations or less effective load distribution. The Hexagon sample (0.35) shows good wear resistance, attributed to its efficient packing and structural stability, which help minimize deformation and evenly distribute stress. The error bars indicate the variability in these measurements, highlighting the consistency and reliability of the data. Overall, the Grid structure demonstrates the best wear resistance, while the Line and Cubic structures show higher wear coefficients and the hexagonal structure provides balanced performance with good wear resistance.

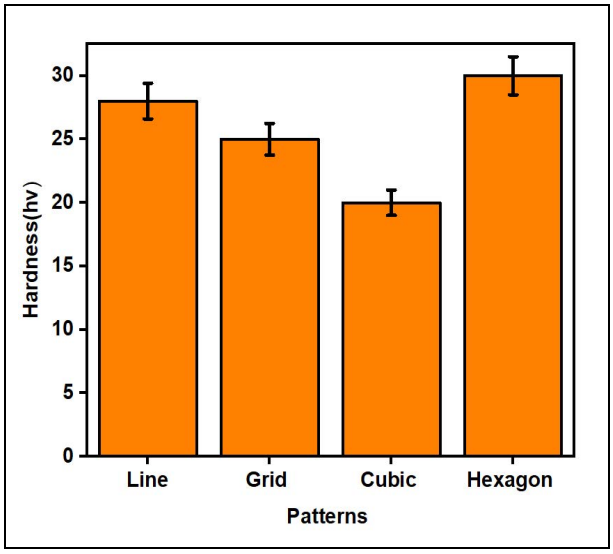

Fig. 5: Variation of hardness against the different patterns of PEEK specimen

3.2 Hardness Test

Fig. 5 shows the microhardness value of the four different patterns of the PEEK specimens. The hardness values of the specimens were recorded after conducting tests as 28HV, 25HV, 20HV, and 30HV for Line, Grid, Cubic, and Hexagon patterns respectively. From the graph, it is observed that the hardness value of the specimens Line and Hexagon pattern was greatly increased by 34% compared to the sample with the cubic pattern. Based on the overall results, it was noted that the specimens with line and hexagon patterns improved the hardness maximum due to the geometrical shape of the patterns.

3.3 SEM Analysis

The scanning electron microscopic images were taken at the wear surfaces of the four different sample patterns such as (a) Line, (b) Grid, (c) Cubic and (d) Hexagon respectively as shown in Fig. 6.

The PEEK material's SEM pictures show a number of surface characteristics that could shed light on its properties and possible functionality. The smooth surface with few pores and a possible break is shown in Fig. 6(a). indicates that although the material is largely undamaged, it may have been subjected to localized stress or impact, and little cracks could eventually cause the material to deteriorate. A more textured surface with deeper pores and fissures is seen in Fig. 6(b), suggesting that the material has seen more stress or degradation, maybe as a result of wear, fatigue, or exposure to the environment, making it more prone to failure. The ridge-

like structure in Figure 6(C) may have developed as a result of material deformation under stress, with cracks or discontinuities inside the ridge indicating weak areas that could weaken the material overall, particularly if the ridge is essential for structural The uneven material properties, which are probably the result of inconsistent processing or different environmental conditions, are shown in Fig. 6.(d), which shows a mix of smooth and rough regions with a higher concentration of pores in some areas. This could lead to localized weakness and increase the likelihood of failure in those regions. Collectively, these pictures show different levels of material deterioration, from little imperfections to more serious structural deficiencies, emphasizing how crucial it is to find and fix flaws in order to stop additional harm. Numerous factors, like the production process, material deterioration, or mechanical stress during service, may have an impact on these characteristics. For example, residual stresses or surface roughness may be left behind by the processing methods used to make the PEEK material, such as injection molding or milling. Furthermore, environmental elements.

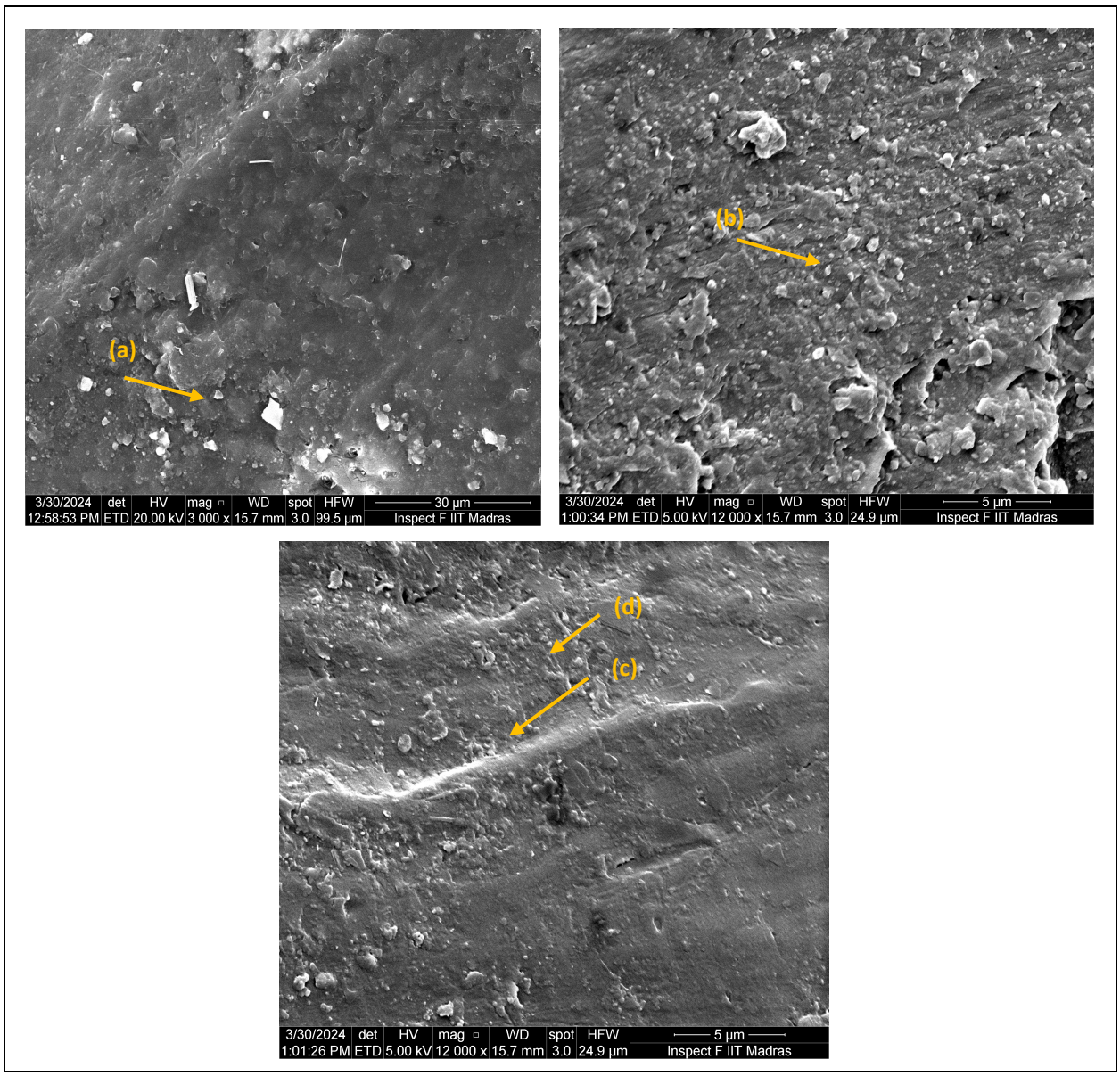

Fig. 6: SEM images of all four patterns of wear test specimens (a) Line (b) Grid (c) Cubic (d) Hexagon

4. CONCLUSION

This research highlights the significant impact of surface patterns on the wear characteristics, coefficient of friction, and hardness of 3D-printed PEEK materials under dynamic loading conditions. The Hexagon pattern demonstrated the highest hardness value and the least wear loss, indicating superior resistance to wear and surface degradation. The hexagon pattern's superior wear resistance and hardness can be attributed to its geometric

design, which provides isotropic load distribution and enhanced stress dissipation during wear tests. The interconnected structure of hexagons offers inherent stability and minimizes localized deformation. This section will be expanded to provide a thorough analysis of the structural mechanics that lead to these properties, supported by references to similar studies in additive manufacturing. The Line pattern also showed low wear loss and high hardness, making it an excellent choice for applications requiring durability. The Grid pattern exhibited the lowest coefficient of friction, suggesting it is ideal for applications where low resistance to movement is crucial. Conversely, the Cubic pattern, despite its highest wear loss and coefficient of friction, provides valuable insights into the trade-offs between wear resistance and friction. SEM images further confirmed the superior wear resistance of the hexagon pattern, revealing minimal surface degradation compared to the other patterns. These findings offer valuable guidance for optimizing surface patterns in engineering and industrial applications, enabling the selection of the most suitable pattern to enhance performance and durability. Future research could extend these findings by exploring additional surface patterns and varying dynamic conditions to further refine the application of 3D-printed PEEK materials in load-bearing environments.

FUNDING

This research received no specific grant from any funding agency in the public, commercial, or not-for-profit sectors.

CONFLICTS OF INTEREST

The authors declare that there is no conflict of interest.

COPYRIGHT

REFERENCES

Chithambaram, K. and Senthilnathan, N., Effects of printing parameters on hardness and wear characteristics of 3D printed polyetheretherketone (PEEK) polymer, *Mater. Lett.*, 356, 135588 (2024). https://doi.org/10.1016/j.matlet.2023.135588

Dhakal, N., Espejo, C., Morina, A. and Emami, N., Tribological performance of 3D printed neat and carbon fiber reinforced PEEK composites, *Tribol. Int.*, 193, 109356 (2024). https://doi.org/10.1016/j.triboint.2024.109356

Durga, R. K. V., Ganesh, N., Yaswanth Kalyan Reddy, S., Mishra, H. and Teja Naidu, T. M. V. P., Experimental research on the mechanical characteristics of fused deposition modelled ABS, PLA and PETG specimens printed in 3D, *Mater Today Proc*., (2023). https://doi.org/10.1016/j.matpr.2023.06.343

Farrugia, J., Vella, P. and Rochman, A., Combining 3D printing and injection moulding for the fabrication of polymer micro-components with internal hollow features, *Prog. Addit. Manuf.*, 9(5), 1353–1364 (2024). https://doi.org/10.1007/s40964-024-00616-x

Greco, A., De Luca, A., Gerbino, S., Lamanna, G., and Sepe, R., Influence of infill pattern and layer height on surface characteristics and fatigue behaviour of FFF-printed PEEK, *Fatigue Fract. Eng. Mater. Struct*., 47(12), 4741–4754 (2024). https://doi.org/10.1111/ffe.14450

Haleem, A. and Javaid, M., Polyether ether ketone (PEEK) and its manufacturing of customised 3D printed dentistry parts using additive manufacturing, *Clin. Epidemiol. Glob. Heal.*, 7(4), 654–660 (2019). https://doi.org/10.1016/j.cegh.2019.03.001

Hassan, M. R., Jeon, H. W., Kim, G. and Park, K., The effects of infill patterns and infill percentages on energy consumption in fused filament fabrication using CFR-PEEK, *Rapid Prototyping J.*, 27(10), 1886–1899 (2021). https://doi.org/10.1108/rpj-11-2020-0288

He, Y., Shen, M., Wang, Q., Wang, T. and Pei, X., Effects of FDM parameters and annealing on the mechanical and tribological properties of PEEK, *Compos. Struct.*, 313, 116901 (2023). https://doi.org/10.1016/j.compstruct.2023.116901

Hou, B., Ren, L., Sun, Y., Zhang, M. and Zhang, H., Structure and properties of heat-resistant ABS resins innovated via MSAMI random copolymer, *J. Thermoplast. Compos. Mater.*, 36(3), 1004–1016 (2023). https://doi.org/10.1177/08927057211044191

Kantaros, A., Soulis, E., Petrescu, F. I. T. and Ganetsos, T., Advanced Composite Materials Utilized in FDM/FFF 3D Printing Manufacturing Processes: The Case of Filled Filaments, *Materials (Basel)*, 16(18), 6210 (2023). https://doi.org/10.3390/ma16186210

Khan, F., Hossain, N., Mim, J. J., Rahman, S. M., Iqbal, M. J., Billah, M. and Chowdhury, M. A., Advances of composite materials in automobile applications – A review, *J. Eng. Res.*, (2024). https://doi.org/10.1016/j.jer.2024.02.017

Khan, S. and Iqbal, A., Organic polymers revolution: Applications and formation strategies, and future perspectives, *J. Polym. Sci. Eng.*, 6(1), 3125 (2023). https://doi.org/10.24294/jpse.v6i1.3125

Kharmanda, G., Challenges and Future Perspectives for Additively Manufactured Polylactic Acid Using Fused Filament Fabrication in Dentistry, *J. Funct. Biomater.*, 14(7), 334 (2023). https://doi.org/10.3390/jfb14070334

Lv, X., Pei, X., Yang, S., Zhang, Y., Wang, Q. and Wang, T., Tribological behavior of PEEK based composites with alternating layered structure fabricated via fused deposition modeling, *Tribol. Int.*, 199, 109953 (2024). https://doi.org/10.1016/j.triboint.2024.109953

Massocchi, D., Riboni, G., Lecis, N., Chatterton, S. and Pennacchi, P., Tribological Characterization of Polyether Ether Ketone (PEEK) Polymers Produced by Additive Manufacturing for Hydrodynamic Bearing Application, *Lubricants*, 9(11), 112 (2021). https://doi.org/10.3390/lubricants9110112

Mehtedi, M. El, Buonadonna, P., Mohtadi, R. El, Aymerich, F. and Carta, M., Surface quality related to machining parameters in 3D-printed PETG components, *Procedia Comput. Sci.*, 232, 1212–1221 (2024). https://doi.org/10.1016/j.procs.2024.01.119

Mrówka, M., Machoczek, T., Jureczko, P., Joszko, K., Gzik, M., Wolański, W. and Wilk, K., Mechanical, Chemical, and Processing Properties of Specimens Manufactured from Poly-Ether-Ether-Ketone (PEEK) Using 3D Printing, *Materials (Basel)*, 14(11), 2717 (2021). https://doi.org/10.3390/ma14112717

Pulipaka, A., Gide, K. M., Beheshti, A. and Bagheri, Z. S., Effect of 3D printing process parameters on surface and mechanical properties of FFF-printed PEEK, *J. Manuf. Processes*, 85, 368–386 (2023). https://doi.org/10.1016/j.jmapro.2022.11.057

Ree, B. J., Critical review and perspectives on recent progresses in 3D printing processes, materials, and applications, *Polymer (Guildf)*, 308, 127384 (2024). https://doi.org/10.1016/j.polymer.2024.127384

Sarker, A., Mondal, S. C., Ahmmed, R., Rana, J., Waheda Rahman Ansary, M. and Bilal, M., Prospects and challenges of polymer nanocomposites for innovative food packaging, In: Smart Polymer Nanocomposites. Elsevier, 355–377 (2023). https://doi.org/10.1016/B978-0-323-91611-0.00021-9

Subramani, R., Mustafa, M. A., Ghadir, G. K., Al-Tmimi, H. M., Alani, Z. K., Haridas, D., Rusho, M. A., Rajeswari, N., Rajan, A. J. and Kumar, A. P., Advancements in 3D printing materials: A comparative analysis of performance and applications, *Appl. Chem. Eng.*, 3867 (2024). https://doi.org/10.59429/ace.v7i2.3867

Timoumi, M., Barhoumi, N., Znaidi, A., Maazouz, A. and Lamnawar, K., Mechanical behavior of 3D-printed PEEK and its application for personalized orbital implants with various infill patterns and densities, *J. Mech. Behav. Biomed. Mater.*, 136, 105534 (2022). https://doi.org/10.1016/j.jmbbm.2022.105534

Wang, X., Hu, J., Liu, J., Liang, Y., Wu, L., Geng, T., Liu, S. and Guo, Y., Tribological Performance and Enhancing Mechanism of 3D Printed PEEK Coated with In Situ ZIF-8 Nanomaterial, *Polymers (Basel)*, 16(8), 1150 (2024). https://doi.org/10.3390/polym16081150

Zhang, Y., Yang, B., Peng, S., Zhang, Z., Cai, S., Yu, J., Wang, D. and Zhang, W., Mechanistic insights into chemical conditioning on transformation of dissolved organic matter and plant biostimulants production during sludge aerobic composting, *Water Res.*, 255, 121446 (2024). https://doi.org/10.1016/j.watres.2024.121446